H.E.S.S. observations of the globular clusters NGC 6388 and M 15 and search for a Dark Matter signal

HESS Collaboration: A. Abramowski[1], F. Acero[2], F. Aharonian[3,4,5], A.G. Akhperjanian[6,5], G. Anton[7], A. Balzer[7], A. Barnacka[8,9], U. Barres de Almeida[10,*], A.R. Bazer-Bachi[11], Y. Becherini[12,13], J. Becker [14], B. Behera[15], K. Bernlöhr[3,16], A. Bochow[3], C. Boisson[17], J. Bolmont[18], P. Bordas[19], V. Borrel[11], J. Brucker[7], F. Brun[13], P. Brun[9], T. Bulik[20], I. Büsching[21], S. Carrigan[3], S. Casanova[3,14], M. Cerruti[17], P.M. Chadwick[10], A. Charbonnier[18], R.C.G. Chaves[3], A. Cheesebrough[10], L.-M. Chounet[13], A.C. Clapson[3], G. Coignet[22], J. Conrad[23], M. Dalton[16], M.K. Daniel[10], I.D. Davids[24], B. Degrange[13], C. Deil[3], H.J. Dickinson[23], A. Djannati-Ataï[12], W. Domainko[3], L.O'C. Drury[4], F. Dubois[22], G. Dubus[25], J. Dyks[8], M. Dyrda[26], K. Egberts[27], P. Eger[7], P. Espigat[12], L. Fallon[4], C. Farnier[2], S. Fegan[13], F. Feinstein[2], M.V. Fernandes[1], A. Fiasson[22], G. Fontaine[13], A. Förster[3], M. Füßling[16], Y.A. Gallant[2], H. Gast[3], L. Gérard[12], D. Gerbig[14], B. Giebels[13], J.F. Glicenstein[9,‡], B. Glück[7], P. Goret[9], D. Göring[7], S. Häffner [7], J.D. Hague [3], D. Hampf[1], M. Hauser[15], S. Heinz[7], G. Heinzelmann[1], G. Henri[25], G. Hermann[3], J.A. Hinton[28], A. Hoffmann[19], W. Hofmann[3], P. Hofverberg[3], M. Holler[7], D. Horns[1], A. Jacholkowska[18], O.C. de Jager[21], C. Jahn[7], M. Jamrozy[29], I. Jung[7], M.A. Kastendieck[1], K. Katarzyński[30], U. Katz[7], S. Kaufmann[15], D. Keogh[10], D. Khangulyan[3], B. Khélifi[13], D. Klochkov[19], W. Kluźniak[8], T. Kneiske[1], Nu. Komin[22], K. Kosack[9], R. Kossakowski[22], H. Laffon[13], G. Lamanna[22], D. Lennarz[3], T. Lohse[16], A. Lopatin[7], C.-C. Lu[3], V. Marandon[12], A. Marcowith[2], J. Masbou[22], D. Maurin[18], N. Maxted[31], T.J.L. McComb[10], M.C. Medina[9], J. Méhault[2], R. Moderski[8], E. Moulin[9,†], C.L. Naumann[18], M. Naumann-Godo[9], M. de Naurois[13], D. Nedbal[32], D. Nekrassov[3], N. Nguyen[1], B. Nicholas[31], J. Niemiec[26], S.J. Nolan[10], S. Ohm[3], J-P. Olive[11], E. de Oña Wilhelmi[3], B. Opitz[1], M. Ostrowski[29], M. Panter[3], M. Paz Arribas[16], G. Pedaletti[15], G. Pelletier[25], P.-O. Petrucci[25], S. Pita[12], G. Pühlhofer[19], M. Punch[12], A. Quirrenbach[15], M. Raue[1], S.M. Rayner[10], A. Reimer[27], O. Reimer[27], M. Renaud[2], R. de los Reyes[3], F. Rieger[3,33], J. Ripken[23], L. Rob[32], S. Rosier-Lees[22], G. Rowell[31], B. Rudak[8], C.B. Rulten[10], J. Ruppel[14], F. Ryde[34], V. Sahakian[6,5], A. Santangelo[19], R. Schlickeiser[14], F.M. Schöck[7], A. Schulz[7], U. Schwanke[16], S. Schwarzburg[19], S. Schwemmer[15], M. Sikora[8], J.L. Skilton[35], H. Sol[17], G. Spengler[16], Ł. Stawarz[29], R. Steenkamp[24], C. Stegmann[7], F. Stinzing[7], K. Stycz[7], I. Sushch[16,**], A. Szostek[29,25], J.-P. Tavernet[18], R. Terrier[12], O. Tibolla[3], M. Tluczykont[1], K. Valerius[7], C. van Eldik[3], G. Vasileiadis[2], C. Venter[21], J.P. Vialle[22], A. Viana[9], P. Vincent[18], M. Vivier[9], H.J. Völk[3], F. Volpe[3], S. Vorobiov[2], M. Vorster[21], S.J. Wagner[15], M. Ward[10], A. Wierzcholska[29], M. Zacharias[14], A. Zajczyk[8], A.A. Zdziarski[8], A. Zech[17], H.-S. Zechlin[1]

---

[1] Universität Hamburg, Institut für Experimentalphysik, Luruper Chaussee 149, D 22761 Hamburg, Germany

[2] Laboratoire de Physique Théorique et Astroparticules, Université Montpellier 2, CNRS/IN2P3, CC 70, Place Eugène Bataillon, F-34095 Montpellier Cedex 5, France

[3] Max-Planck-Institut für Kernphysik, P.O. Box 103980, D 69029 Heidelberg, Germany

[4] Dublin Institute for Advanced Studies, 31 Fitzwilliam Place, Dublin 2, Ireland

[5] National Academy of Sciences of the Republic of Armenia, Yerevan

[6] Yerevan Physics Institute, 2 Alikhanian Brothers St., 375036 Yerevan, Armenia

[7] Universität Erlangen-Nürnberg, Physikalisches Institut, Erwin-Rommel-Str. 1, D 91058 Erlangen, Germany

[8] Nicolaus Copernicus Astronomical Center, ul. Bartycka 18, 00-716 Warsaw, Poland

[9] IRFU/DSM/CEA, CE Saclay, F-91191 Gif-sur-Yvette, Cedex, France

[10] University of Durham, Department of Physics, South Road, Durham DH1 3LE, U.K.

[11] Centre d'Etude Spatiale des Rayonnements, CNRS/UPS, 9 av. du Colonel Roche, BP 4346, F-31029 Toulouse Cedex 4, France

[12] Astroparticule et Cosmologie (APC), CNRS, Université Paris 7 Denis Diderot, 10, rue Alice Domon et Leonie Duquet, F-75205 Paris Cedex 13, France. Also at UMR 7164 (CNRS, Université Paris VII, CEA, Observatoire de Paris)

[13] Laboratoire Leprince-Ringuet, Ecole Polytechnique, CNRS/IN2P3, F-91128 Palaiseau, France

[14] Institut für Theoretische Physik, Lehrstuhl IV: Weltraum und Astrophysik, Ruhr-Universität Bochum, D 44780 Bochum, Germany

[15] Landessternwarte, Universität Heidelberg, Königstuhl, D 69117 Heidelberg, Germany

[16] Institut für Physik, Humboldt-Universität zu Berlin, Newtonstr. 15, D 12489 Berlin, Germany

[17] LUTH, Observatoire de Paris, CNRS, Université Paris Diderot, 5 Place Jules Janssen, 92190 Meudon, France

[18] LPNHE, Université Pierre et Marie Curie Paris 6, Université Denis Diderot Paris 7, CNRS/IN2P3, 4 Place Jussieu, F-75252, Paris Cedex 5, France

[19] Institut für Astronomie und Astrophysik, Universität Tübingen, Sand 1, D 72076 Tübingen, Germany

[20] Astronomical Observatory, The University of Warsaw, Al. Ujazdowskie 4, 00-478 Warsaw, Poland

[21] Unit for Space Physics, North-West University, Potchefstroom 2520, South Africa

[22] Laboratoire d'Annecy-le-Vieux de Physique des Particules, CNRS/IN2P3, 9 Chemin de Bellevue - BP 110 F-74941 Annecy-le-Vieux Cedex, France

[23] Oskar Klein Centre, Department of Physics, Royal Institute of Technology (KTH), Albanova, SE-10691 Stockholm, Sweden

[24] University of Namibia, Department of Physics, Private Bag 13301, Windhoek, Namibia

[25] Laboratoire d'Astrophysique de Grenoble, INSU/CNRS, Université Joseph Fourier, BP 53, F-38041 Grenoble Cedex 9, France

[26] Instytut Fizyki Jądrowej PAN, ul. Radzikowskiego 152, 31-342 Kraków, Poland

[27] Institut für Astro- und Teilchenphysik, Leopold-Franzens-Universität Innsbruck, A-6020 Innsbruck, Austria

Abstract

Observations of the globular clusters NGC 6388 and M 15 were carried out by the H.E.S.S. array of Cherenkov telescopes for a live time of 27.2 and 15.2 hours respectively. No gamma-ray signal is found at the nominal target position of NGC 6388 and M 15. In the primordial formation scenario, globular clusters are formed in a dark matter halo and dark matter could still be present in the baryon-dominated environment of globular clusters. This opens the possibility of observing a dark matter self-annihilation signal. The dark matter content of the globular clusters NGC 6388 and M 15 is modelled taking into account the astrophysical processes that can be expected to influence the dark matter distribution during the evolution of the globular cluster: the adiabatic contraction of dark matter by baryons, the adiabatic growth of a black hole in the dark matter halo and the kinetic heating of dark matter by stars. 95% confidence level exclusion limits on the dark matter particle velocity-weighted annihilation cross section are derived for these dark matter haloes. In the TeV range, the limits on the velocity-weighted annihilation cross section are derived at the $10^{-25}\,\mathrm{cm^3s^{-1}}$ level and a few $10^{-24}\,\mathrm{cm^3s^{-1}}$ for NGC 6388 and M 15 respectively.

Subject headings: Gamma-rays : observations, Globular clusters, Black Holes, Dark Matter

---

[28] Department of Physics and Astronomy, The University of Leicester, University Road, Leicester, LE1 7RH, United Kingdom

[29] Obserwatorium Astronomiczne, Uniwersytet Jagielloński, ul. Orla 171, 30-244 Kraków, Poland

[30] Toruń Centre for Astronomy, Nicolaus Copernicus University, ul. Gagarina 11, 87-100 Toruń, Poland

[31] School of Chemistry & Physics, University of Adelaide, Adelaide 5005, Australia

[32] Charles University, Faculty of Mathematics and Physics, Institute of Particle and Nuclear Physics, V Holešovičkách 2, 180 00 Prague 8, Czech Republic

[33] European Associated Laboratory for Gamma-Ray Astronomy, jointly supported by CNRS and MPG

[34] Oskar Klein Centre, Department of Physics, Royal Institute of Technology (KTH), Albanova, SE-10691 Stockholm, Sweden

[35] School of Physics & Astronomy, University of Leeds, Leeds LS2 9JT, UK

[*] supported by CAPES Foundation, Ministry of Education of Brazil

[**] supported by Erasmus Mundus, External Cooperation Window

[†] emmanuel.moulin@cea.fr

[‡] jean-francois.glicenstein@cea.fr

1. Introduction

Dark matter (DM) is expected to play a key role in the dynamics of a wide range of systems, from galactic object scale to galaxy cluster scale (Bertone et al. 2005). The inner parts of galaxies were used extensively to search for DM even though they are not necessarily dominated by DM (Englmaier & Gerhard 2005). Observations by the H.E.S.S. experiment towards the Galactic Center reveal a very high energy (VHE, $E_\gamma \gtrsim 100$ GeV) gamma-ray signal with the flux level $\Phi(> 1\mathrm{TeV}) \simeq 2 \times 10^{-12}\,\mathrm{cm}^{-2}\mathrm{s}^{-1}$ (Aharonian et al. 2009a). The plausible DM-originated fraction of this signal is entirely dominated by standard astrophysical emission processes (Aharonian et al. 2006a). As opposed to this, dwarf galaxies are believed to be among the most DM-dominated objects and are believed to have a reduced astrophysical background (Mateo 1998) since these objects have little or no recent star formation activity. Nearby dwarf galaxies in the Local Group have already been observed with H.E.S.S., *i.e.* Sagittarius, Canis Major, Sculptor and Carina (Aharonian et al. 2008; Aharonian et al. 2009b; Aharonian et al. 2011), yielding no signal. Exclusion limits on the velocity-weighed annihilation cross section between $\sim 10^{-24}$ to $\sim 10^{-22}\,\mathrm{cm}^3\mathrm{s}^{-1}$ have been reported in the TeV range.

Several Galactic Globular Clusters (GCs) have been observed with ground-based Cherenkov telescopes and upper limits on γ-ray emission from standard astrophysical processes have been reported on Omega Centauri, 47 Tucanæ, M 13, M 15 and M 5 (Kabuki et al. 2007; Aharonian et al. 2009b; Anderhub et al. 2009; McCutcheon 2009). GCs are also potential targets for indirect DM searches (Wood et al. 2008). They are dense stellar systems of $\gtrsim$ 10 Gyr old, found in haloes of galaxies, with typical masses between 10^4 and a few 10^6 $\mathrm{M}_\odot$, similar to dwarf galaxies. However, GCs are much more compact than dwarf galaxies. Observations of GCs do not suggest the presence of a significant amount of DM, but rather that these objects are dominated by baryons (Binney & Tremaine 1987). In the primordial formation scenario of GCs (Peebles 1984), GCs were formed in DM minihaloes before or during the reionization (Komatsu et al. 2009), before formation of galaxies. However the distribution of GC colors (Brodie & Strader 2006) suggests that only metal poor clusters have a cosmological origin while metal rich clusters formed in star-forming events such as galaxy-galaxy mergers. The existence of an extended dark halo required by the GC primordial formation scenario, has been challenged recently by Baumgardt et al. (2009) and Conroy et al. (2010). They show that the stellar kinematics of NGC 2419, a remote GC which experiences little tidal effects from the Milky Way, is incompatible with the presence of an extended dark halo. However, Cohen et al. (2010) have shown that the measured spread in the Ca abundance can be only explained if NGC 2419 is the remnant of a more massive object.

In the purpose of the paper, GCs are assumed to have formed in DM minihaloes and thus were DM-dominated in their primordial stage. Note that M 15 is a metal-poor GC, [Fe/H]$\simeq$-2.37 (Harris 1996), while NGC 6388 is metal-rich, [Fe/H]$\simeq$-0.55 (Harris 1996), so the DM minihalo scenario is better motivated for M 15 than NGC 6388. However, NGC 6388 might host a $\gtrsim 10^3\,\mathrm{M}_\odot$ black hole (Lanzoni et al. 2007). Such massive ($\gtrsim 10^3$ $\mathrm{M}_\odot$) black holes are not easily formed in star-forming events (Yungelson et al. 2008) suggesting a primordial formation origin. During the evolution of the globular cluster, the DM reacts to the infall of baryons and is pulled in towards the center. This process is usually referred to as the adiabatic contraction (AC) model (Blumenthal et al. 1986; Zeldovich et al. 1980; Jesseit et al. 2002; Gnedin et al. 2004; Prada et al. 2004). The effect of the contraction of DM in response to the baryon infall is particularly important for the calculation of the DM annihilation in baryonic environments such as the Galactic Center region (Gnedin & Primack 2004; Prada et al. 2004).

The distribution of baryons and DM is affected by the kinetic heating of DM by baryons (Merritt 2004) and by the presence of a black hole (BH) (Gondolo & Silk 1999). A growing body of observations on GCs shows that they may harbor intermediate mass black holes (IMBHs) with masses ranging from 10^3 to 10^5 $M_\odot$, although the existence of these objects is not yet established. Indirect evidence includes the extrapolation of the empirical relation M_{BH}-M_{Bulge} found for the supermassive BHs in galactic nuclei, which leads naturally to the prediction of existence of IMBHs (Magorrian et al. 1998). Besides, ultra-luminous X-ray sources (ULXs) apparently not associated to active galactic nuclei are proposed to be related to IMBHs (Colbert & Ptak 2002; Swartz et al. 2004; Dewangan et al. 2005). From the theoretical side, the existence of IMBHs is a generic assumption of scenarios that seek to explain the formation of supermassive BHs from the accretion and merging of massive seeds (Islama et al. 2003; Volonteri et al. 2003; Koushiappas et al. 2004). Several globular clusters may host IMBHs: NGC 6388 (Lanzoni et al. 2007), ω Centauri (Noyola et al. 2008) in the Milky Way or even G1 in M 31 (Kong 2007; Ulvestad et al. 2007).

The paper is structured as follows. Section 2 describes the observations carried out with the H.E.S.S. experiment and the analysis of the data on the two Galactic GCs NGC 6388 and M 15. In section 3, the DM halo modelling relevant for the two GCs is briefly presented (more details are given in the appendix) and exclusion limits on the velocity-weighted annihilation cross section of DM particles are derived for realistic DM halo profiles. Finally, the results are summarized in section 4.

2. Observations and data analysis

The H.E.S.S. (High Energy Stereoscopic System) array of Cherenkov telescopes is located in the Khomas Highland of Namibia at an altitude of 1800 m above sea level. The system consists of four Imaging Atmospheric Cherenkov telescopes of 12 m diameter ($\sim$107 m^2) each. The total field of view of H.E.S.S. is 5° in diameter. The H.E.S.S. instrument achieves an angular resolution of 5' per gamma-ray and a point-like source sensitivity at the level of $10^{-13}\,\mathrm{cm}^{-2}\mathrm{s}^{-1}$ above 1 TeV for a 5σ detection in 25 hours at an observation zenith angle of 20° (de Naurois & Rolland 2009).

For both M 15 and NGC 6388, data are taken in *wobble mode* (Aharonian et al. 2006b), where the pointing direction is chosen at an alternating offset of $\pm0.7°$ to $\pm1.0°$ from the target position. Standard quality selection (Aharonian et al. 2006b) is applied to the data. After the calibration of the raw data from PMT signals, the events are reconstructed using a technique based on a semianalytical shower development model (de Naurois & Rolland 2009). This reconstruction method yields a relative energy resolution of ~10% and an angular resolution of 0.06° per gamma-ray (68% containment radius). The background level is estimated using the ring-background method (Pühlhofer et al. 2003; Berge et al. 2007). The core of the GCs is very small in comparison to the H.E.S.S. point spread function. They would thus be seen as point sources by H.E.S.S.. The source region referred to hereafter as the ON region, is defined as a circular region of 0.07°radius around the target position. The background region is defined as an annulus around the pointing position with a medium radius equal to the distance of the target and a half-thickness of 0.07°. It is referred to hereafter as the OFF region. The cut values used to select the gamma-ray events are shown in Tab. 1. Given the Galactic latitude of the two Galactic GCs, contamination by diffuse TeV gamma-ray emission is very unlikely. The results presented below have been cross-checked by an independent analysis chain (Berge et al. 2007; Aharonian et al. 2005). Both analyses give consistent results.

2.1. NGC 6388

NGC 6388 is one of the best known Galactic GC. It is located at ~ 11.5 kpc from the Sun, at RA $= 17^{\rm h}36^{\rm m}17.05^{\rm s}$ and Dec $= -44°44'05.8''$ (J2000), and has a mass estimated to be $\sim 10^6$ M$_\odot$. The stellar mass density in the core, with radius $r_{\rm c} = 0.4$ pc (0.12 arcminutes), reaches $\sim 5{\times}10^5$ M$_\odot$pc^{-3}. The tidal radius is $r_{\rm t} \sim 25$ pc (Lanzoni et al. 2007). The structural properties of NGC 6388 are summarized in Tab. 2. Using the high-resolution HST and WFI observations at ESO, Lanzoni et al.(2007) show that the surface brightness density of stars significantly deviates from a flat core in the inner part, which is compatible with the existence of an IMBH with a mass of $\sim 5\times10^3$ M$_\odot$. A power law with a slope of -0.2 is detected in the surface brightness density profile, which suggests the presence of a central IMBH (Baumgardt et al. 2005; Noyola & Gebhardt 2006; Umbreit et al. 2008). The *Chandra* satellite has detected three X-ray sources, coincident in position with the centre of gravity of NGC 6388 located with an uncertainty of 0.3″. One of these may be the X-ray counterpart of the putative IMBH (Nucita et al.2007).

The H.E.S.S. observations of NGC 6388 were taken between June 2008 and July 2009. The observation zenith angles range from 20° to 44° with a mean zenith angle of 22.9°, and the exposure time is 27.2 hours. The left-hand side of Fig. 1 shows the θ^2 radial distribution of the ON and OFF events for NGC 6388. $\rm N_{ON} = 71$ gamma-ray candidates were found in the ON region while the measured number of OFF events is $\rm N_{OFF} = 1754$. With the ratio of the off-source solid angle region to the on-source solid angle region $\alpha = 26.5$, the expected number of background events in the ON region is 66.1. Since $\rm N_{ON}$ and $\rm N_{OFF}/\alpha$ are compatible at the 2σ level, no significant gamma-ray excess is found above the background. An upper limit at 95% confidence level (C.L.) on the number of gamma-rays can be derived using the method developed in Rolke et al.(2005): $\rm N_\gamma^{95\%C.L.} = 21.6$.

2.2. M 15

M 15 (NGC 7078) is a well-studied Galactic GC centered at the position RA = $21^{\rm h}28^{\rm m}58.3^{\rm s}$ and Dec = $12^\circ10'00.6''$ (J2000). It is situated at $\sim 10\,$kpc from the Sun. Its estimated mass is $\sim 5\times10^5\,{\rm M}_\odot$. The stellar mass density in the core with radius $r_{\rm c}$ = 0.04 pc is about $10^7\,{\rm M}_\odot{\rm pc}^{-3}$ (Dull et al.1997), and the tidal radius is $r_{\rm t} \sim 30\,$pc. The structural properties of M 15 are summarized in Tab. 2. The surface brightness density of the GC M 15 suggests the presence of a stellar cusp in the inner part, at least down to distances of a few $10^{-2}\,$pc (Dull et al.1997). M 15 may thus harbor an IMBH (Gerssen et al. 2002; Kiselev et al. 2008) in its center. However, the study on milli-second pulsars in M 15 sets an upper limit of $10^3\,{\rm M}_\odot$ on the mass of a hypothetical central BH (De Paolis et al. 1996). In what follows, no central back hole is assumed for the modelling of M 15.

The observations of M 15 by H.E.S.S. were carried out in 2006 and 2007 with an offset angle of 0.7° and zenith angles from 34° to 44° resulting in 15.2 hours of high quality data at a mean zenith angle of 37.0°. The right-hand side of Fig. 1 shows the θ^2 radial distribution of the ON and OFF events for M 15. The data analysis reveals no significant gamma-ray signal at the nominal position. With $\rm N_{ON}$ = 28, $\rm N_{OFF}$ = 719 and α = 26.6, the expected number of background events in the ON region is 27.0. The 95% C.L. upper limit on the number of gamma-rays is $\rm N_\gamma^{95\%C.L.}$ = 11.5. Tab. 3 summarizes observations and upper limits on count numbers for NGC 6388 and M 15.

3. Dark matter constraints

3.1. Dark matter halo modelling

The relaxation time, defined in Eq. (A1) of the appendix, has a much smaller value, $T_r \sim 10^7\,$yr, in GCs than in galaxies, where it is typically of the order of 10^{13} yr (Binney & Tremaine 1987). Since GCs are among the oldest objects known, their present DM density depends on their history and evolution. During infall events such as core collapses (Spitzer 1987), the DM is compressed towards the center following the AC scenario (Zeldovich et al. 1980; Blumenthal et al. 1986). This profile is referred to hereafter as the AC NFW profile. But the kinetic heating of DM particles by stars (Merritt 2004) tends to wash out the adiabatic contraction effect over a timescale of the order of $\rm T_r$. Both effects were taken into account in the modelling of M 15 and NGC 6388, following the approach of Merritt et al. (2007) and Bertone & Fairbarn (2008).

As mentioned in the introduction, the primordial formation scenario of globular clusters (Peebles 1984) assumed here requires that globular clusters were formed in extended DM haloes. The DM halo profile of a globular cluster is thus modelled assuming an initial Navarro-Frenk-White (NFW) profile (Navarro et al. 1997) described by:

$$\rho(r) = \rho_0 \left(\frac{r}{r_{\rm s}}\right)^{-1} \left(1+\frac{r}{r_{\rm s}}\right)^{-2} . \tag{1}$$

This DM halo is parameterized by a virial mass[1] $M_{\rm vir}$ and a concentration parameter $c_{\rm vir}$. The normalization parameter ρ_0 and the scale radius $r_{\rm s}$ can be related to the virial mass and the concentration parameter using the following relations (Navarro et al. 1997)

$$\rho_0 = \frac{M_{\rm vir}}{4\pi r_{\rm s}^3 f(c_{\rm vir})} \quad , \quad r_{\rm s} = \frac{R_{\rm vir}}{c_{\rm vir}} \ ; \tag{2}$$

where the function $f(x)$ is, neglecting constants, the volume integral of the NFW profile given by $f(x) \equiv \ln(1+x) - x/(1+x)$. The present baryonic mass of the GC provides a lower bound on its virial mass. Besides, for $M_{\rm vir}$ larger than 10^8 $\rm M_\odot$ the GC would be expected to spiral towards the center of the Milky Way in less than the age of the Universe. Conservative values for $M_{\rm vir}$ lie therefore in the range $[5 \times 10^6 - 5 \times 10^7]$ $\rm M_\odot$ (Wood et al.2008), corresponding[2] to $\rm c_{vir}$ between ∼48 and 65. In this paper, initial DM haloes of GCs are modelled with $\rm M_{vir} = 10^7$ $\rm M_\odot$. The value of $c_{\rm vir}$ used in the model of NGC 6388 is calculated from the formula of Bullock et al. (2001). For M 15, the value of $c_{\rm vir}$ is taken from Wood et al.(2008). Both values are listed in Tab. 4.

The presence of a central BH changes the DM and stellar densities in regions where the BH dominates the gravitational potential, *i.e.* for distances to the BH lower than the radius of gravitational influence $r_{\rm h}$[3]. The adiabatic growth of the BH leads to a spiked DM distribution with an index of 9/4 for an initial DM distribution with an index of 1, as for the NFW profile. This profile is referred to as the IMBH NFW profile. The spike is smoothed by the kinetic heating of DM by stars over the timescale $T_{\rm r}$, forming a density profile proportional to $\rm r^{-3/2}$ called DM crest (Merritt et al. 2007), which corresponds to the final profile.

The dark halo models of M 15 and NGC 6388 are described in details in the appendix. The DM halo of M 15 differs from the model published in Wood et al. (2008), since the effect of dark matter heating by stars is considered in addition to the effect of adiabatic contraction. The inferred DM mass densities of NGC 6388 and M 15 are shown in Fig. 2 and Fig. 3 respectively.

3.2. Dark matter annihilation signal

The gamma-ray flux expected from DM annihilations can be decomposed into an astrophysical term and a particle physics term as (Bertone et al. 2005):

$$\frac{{\rm d}\Phi(\Delta\Omega, E_\gamma)}{{\rm d}E_\gamma} = \frac{1}{8\pi} \underbrace{\frac{\langle \sigma v \rangle}{m_{\rm DM}^2} \frac{{\rm d}N_\gamma}{{\rm d}E_\gamma}}_{Particle\,Physics} \times \underbrace{\bar{J}(\Delta\Omega)\Delta\Omega}_{Astrophysics} \ . \tag{3}$$

---

[1] $\rm M_{vir}$ is defined as the mass inside the radius $\rm R_{vir}$ assuming a mean density equal to 200 times the critical density of the Universe (Amsler et al. 2009).

[2] $\rm M_{vir}$ and $\rm c_{vir}$ are strongly correlated (Navarro et al. 1997, Bullock et al. 2001). In Bullock et al. (2001) , $\rm c_{vir} = 9 \times (M_{vir}/1.5 \times 10^{13} h^{-1} M_\odot)^{-0.13}$ where h is the present day normalized Hubble constant (Amsler et al. 2009).

[3] The radius of gravitational influence of a BH is defined by the equation $\rm M(< r_h) \equiv \int_0^{r_h} \rho(r) d^3r = 2\,M_{BH}$.

The astrophysical factor ($\bar{J}$) is generally expressed as the integral over the line of sight (los) of the squared density averaged over the solid angle $\Delta\Omega$:

$$\bar{J} = \frac{1}{\Delta\Omega}\int_{\Delta\Omega} d\Omega \int_{los} ds\, \rho^2(r(s)) \tag{4}$$

with $r(s) = \sqrt{s^2 + s_0^2 - 2ss_0\cos\theta}$, s_0 the distance of the source from the Sun and θ the opening angle of the integration cone centered on the target position. To match the analysis cuts used in this work (see Section 2), $\Delta\Omega$ is set to 5×10^{-6} sr. Tab. 4 shows the values of the astrophysical factor for the DM halo profiles presented in Sec. 3.1. In the case of the IMBH NFW and final DM profiles for NGC 6388, the calculation of the astrophysical factor requires a minimum cutoff for the integration radius. For the IMBH NFW and final profiles, the integral diverges as $r_{\rm min}^{-3/2}$ and $\log(r_{\rm min}^{-1})$ respectively, where $r_{\rm min}$ is the inner radius. $r_{\rm min}$ is usually taken as $\mathrm{Max}[r_S, r_A]$ where $r_S \equiv 2GM_{\rm BH}/c^2$ is the Schwarzschild radius of the black hole and $r_{\rm A}$ is the self-annihilation radius calculated for an annihilation time of 10 Gyr. Typical values of m_{DM} and $\langle\sigma v\rangle$ give $\mathrm{r_A} \simeq 10^{-5}$ pc so that $r_{\rm min} = r_{\rm A}$. The value of the astrophysical factor for the final profile is insensitive to the assumed value of $r_{\rm min}$. The values for M 15 are calculated using the DM modelling described in Sec. 3.1. The evolution of M 15 leads to a depletion of DM, implying a decrease of $\bar{J}$. In the case of NGC 6388, the effect of the BH in the stellar environment boosts $\bar{J}$ to a value higher than that obtained for the initial NFW profile.

3.3. Exclusion limits

The exclusion limits on the particle physics parameters, *i.e.* the DM particle mass $m_{\rm DM}$ and the velocity-weighted annihilation cross section $\langle\sigma v\rangle$, are calculated using the astrophysical factor calculated for each DM halo model by:

$$\langle\sigma v\rangle_{\rm min}^{95\%\ \rm C.L.} = \frac{8\pi}{T_{\rm obs}}\frac{m_{\rm DM}^2}{\bar{J}(\Delta\Omega)\Delta\Omega}\frac{N_\gamma^{95\%\ \rm C.L.}}{\displaystyle\int_0^{m_{\rm DM}} A_{\rm eff}(E_\gamma)\frac{\mathrm{d}N_\gamma}{\mathrm{d}E_\gamma}dE_\gamma} \tag{5}$$

where $\mathrm{d}N_\gamma/\mathrm{d}E_\gamma$ is the DM-produced differential continuum gamma-ray spectrum and $A_{\rm eff}$ is the effective area of the instrument during the observations (Aharonian et al. 2008). Fig. 4 shows the 95% C.L. exclusion limits for NGC 6388 on $\langle\sigma v\rangle$ for the initial NFW (dashed line) and the final profile (solid line) derived from the 95% C.L. upper limit on the number of gamma-rays. The generic parametrization from Bergström (2000) as well as a parametrization including contributions from virtual internal Bremsstrahlung and final state radiation (Bringmann et al. 2008) are used for the differential gamma-ray spectra. The Bergström (2000) parametrization is derived from a fit to the gamma-ray spectrum from WIMP annihilations into W and Z pairs. The latter includes both gamma-rays from virtual particles and from charged particle final states of the pair annihilation of winos (Bertone et al. 2005). The limits are 1 to 3 orders of magnitude above the natural value of the velocity-weighted annihilation cross section for thermally-produced DM (Bertone et al. 2005).

Fig. 5 shows the H.E.S.S. 95% C.L. exclusion limits for M 15 for the initial and final DM profiles, as well as those obtained with the Whipple Cherenkov telescope (blue area) in Wood et al.(2008). The thickness of the drawn lines represents the astrophysical uncertainty induced by the plausible mass range for the initial virial mass. The H.E.S.S. limit reaches $\langle\sigma v\rangle \sim 5\times10^{-23}\,\mathrm{cm^3s^{-1}}$ and $\langle\sigma v\rangle \sim 5\times10^{-24}\,\mathrm{cm^3s^{-1}}$ around $m_{\mathrm{DM}} = 2$ TeV for the initial NFW profile and the final profile respectively. For comparison, the exclusion limit obtained for H.E.S.S. using the DM halo modelling of Wood et al.(2008) are also shown (gray area). Stronger constraints are obtained with H.E.S.S. due to the combination of larger effective area, $3\times10^5\,\mathrm{m^2}$ vs. $5\times10^4\,\mathrm{m^2}$, better angular resolution, 0.06° vs. 0.25°, better upper limit on the number of gamma-rays (11.5 vs. $\sim$ 67.7) and longer observation time (15.2 h vs. 1.2 h).

4. Summary

The present paper gives for the first time exclusion limits on dark matter towards several globular clusters taking into account all relevant astrophysical effects affecting the hypothetical DM halo. The H.E.S.S. observations reveal no significant gamma-ray excess from point-like sources located at the nominal position of the Galactic GCs NGC 6388 and M 15. The hypothetical DM halo has been modelled taking into account possible astrophysical processes leading to substantial changes in the initial DM profile: the adiabatic contraction of DM by baryons and the adiabatic growth of a BH at the center of the DM halo. The scattering of DM by stars in such a dense stellar environment has been taken into account to provide realistic final DM haloes. This effect is of crucial importance to model DM haloes in these baryon-dominated environments and leads to a depletion of DM during the evolution of the globular cluster. On the other hand, the presence of a central massive BH enhances the DM density in the center. The constraints on the velocity-weighted annihilation cross section of the DM particle are derived using DM halo profiles taking into account the above-mentioned astrophysical effects on the initial DM density. They lie at the level of a few $10^{-25}\,\mathrm{cm^3s^{-1}}$ for NGC 6388 in the TeV energy range. Assuming the absence of a massive BH in the center of M 15, the constraints are of the order of a few $10^{-24}\,\mathrm{cm^3s^{-1}}$.

The support of the Namibian authorities and of the University of Namibia in facilitating the construction and operation of H.E.S.S. is gratefully acknowledged, as is the support by the German Ministry for Education and Research (BMBF), the Max Planck Society, the French Ministry for Research, the CNRS-IN2P3 and the Astroparticle Interdisciplinary Programme of the CNRS, the U.K. Particle Physics and Astronomy Research Council (PPARC), the IPNP of the Charles University, the South African Department of Science and Technology and National Research Foundation, and by the University of Namibia. We appreciate the excellent work of the technical support staff in Berlin, Durham, Hamburg, Heildelberg, Palaiseau, Paris, Saclay, and in Namibia in the construction and operation of the equipment.

A. Models of the M 15 and NGC 6388 dark matter halos

A.1. M 15 dark matter halo

The modelling of the M 15 DM halo proceeds in two steps. In the first step, the dark halo is assumed to be adiabatically compressed during the collapse of the core of M 15. The model used for the initial and final baryon and DM densities is described in Wood et al. (2008). The final baryon density is the observed mass density, taken from Gebhardt et al. (1997). The DM is compressed during the baryonic collapse. The timescale for the collapse is $\simeq 100\ T_{\rm r}$, where the relaxation time $T_{\rm r}$ is given by Spitzer (1987):

$$T_{\rm r} = \frac{3.4\times10^9}{\ln\Lambda}\left(\frac{v_{\rm rms}}{\rm kms^{-1}}\right)^3\left(\frac{m}{\rm M_\odot}\right)^{-2}\left(\frac{n}{\rm pc^{-3}}\right)^{-1}{\rm yr}\ . \tag{A1}$$

In Eq. (A1), $v_{\rm rms}$ is the velocity dispersion, n is the stellar density and $\ln\Lambda$ is the usual Coulomb logarithm. In the case of the center of M 15, taking $v_{\rm rms} = 10.2\pm1.4\,{\rm kms^{-1}}$ (Dull et al.1997), $\ln\Lambda = 13.1$ and adopting a typical stellar mass value of $m = 0.4\,{\rm M_\odot}$ (Dull et al.1997), one finds $T_{\rm r} \simeq 7\times10^4$ yr. $T_{\rm r}$ is an increasing function of the distance r to the center of the M 15. For $r \gtrsim r_{\rm heat} = 5\,{\rm pc}$, the relaxation time is larger than the age of the Universe. The central value of $T_{\rm r}$ and the position of $\rm r_{heat}$ have only weak dependencies on the actual values of $v_{\rm rms}$ and n when the latter are varied in their uncertainty ranges. Because of AC, the DM evolution takes place in less than a few orbital periods. The orbital period of a star orbiting the core of M 15 is of the order of 1000 yr, which is much less than $T_{\rm r}$. The AC method should thus be valid. The value of the DM density after AC is similar to the result of Wood et al.(2008), see Fig. 3 and Fig. 7 of Wood et al.(2008). At the same time, the DM is heated up by stellar matter. This process is described in Merritt (2004). DM is scattered by stars in a few $T_{\rm r}$, leading to a depletion of the core. For $r \gtrsim 5\,{\rm pc}$, the DM distribution is not affected by heating. The DM scattering is taken into account with the procedure described in Bertone & Fairbarn (2008) for the M 4 globular cluster. A DM mass density of $\rho_{\rm M15} \sim 35\,{\rm M_\odot pc^{-3}}$ is obtained at the radius where the heating time is comparable to the age of the universe. For $r \lesssim 5$ pc, the DM halo is swept out by heating and the DM mass density was assumed to take the constant $\rho_{\rm M15}$ value. The DM mass density of M 15 called final profile is shown on Fig. 3.

A.2. NGC 6388 dark matter halo

The modelling of the NGC 6388 DM halo also proceeds in two steps. The first step is the AC of the DM halo by the IMBH and baryons. An initial baryon fraction of 20% (Spergel et al. 2007) is assumed with the same spatial distribution like the DM. The AC scenario gives the resulting DM distribution knowing the measured baryonic mass profile. This DM halo profile is called AC NFW profile. The surface density profile of NGC 6388 is well fitted by a modified King model including a black hole, characterized by a core radius $r_{\rm c} = 7.2''$ and a concentration $c = 1.8$ (Lanzoni et al.2007).

Using these parameters, the numerical integration of the Poisson equation yields the behavior of the gravitational potential from which it is straightforward to compute the baryonic density profile. The initial NFW profile is characterized by $\mathrm{M_{vir}} = 10^7\,\mathrm{M_\odot}$. Since the mass of the IMBH is just a small fraction of the total mass in the core of NGC 6388, the dynamics of DM is influenced mainly by baryonic matter, except in the immediate vicinity of the black hole. Using a central velocity dispersion of $v_\mathrm{rms} = 18.9 \pm 0.8$ kms^{-1} (Pryor & Meylan , 1993) and $\ln\Lambda = 14.7$, the central relaxation time is found to be $T_\mathrm{r} \simeq 8\times10^6$ yr. The orbital period of a star orbiting the core of NGC 6388 is 5000 yr, so that the AC method is again valid. The relaxation time is larger than the age of the Universe for $r > r_\mathrm{heat}$. The distribution of the DM density around the black hole (for $\mathrm{r} \lesssim \mathrm{r_h}$) is changing with time, but tends to a power law with index 3/2 after a few T_r. The final DM distribution is thus obtained by extending the prescription of Bertone & Fairbarn (2008). Far from the center of the cluster, the stellar density is low and thus the heating time becomes large so that the DM distribution is unaffected. A mass density of $\sim$140 $\mathrm{M_\odot pc^{-3}}$ is obtained at the radius $r_\mathrm{heat} \sim 4\,\mathrm{pc}$ where the heating time is comparable to the age of the Universe. In the region between $r_\mathrm{h} < r < r_\mathrm{heat}$, the DM density is expected to be described by a smooth curve similar to Fig. 1 of Merritt et al.(2007). In the modelling for NGC 6388, the DM density was conservatively assumed to take a constant value of $140\,\mathrm{M_\odot pc^{-3}}$ in the region $r_\mathrm{h} < r < r_\mathrm{heat}$. For $r < r_\mathrm{h}$, the DM density is given by $\rho(\mathrm{r}) = 140\,\mathrm{M_\odot pc^{-3}}\,(\mathrm{r/r_h})^{-3/2}$. The final profile for the DM distribution of NGC 6388 is shown in Fig. 2. At the position of NGC 6388, the DM density from the smooth Galactic halo assuming a NFW profile is $\sim 0.03\,\mathrm{M_\odot pc^{-3}}$.

REFERENCES

Aharonian, F., *al.* [HESS Collaboration], 2005, A&A, 430, 865

Aharonian, F., *et al.* [HESS Collaboration], 2006a, Phys. Rev. Lett., 97, 221102 [Erratum-ibid. 97, 249901]

Aharonian, F., *et al.* [HESS Collaboration], 2006b, A&A, 457, 899

Aharonian, F., *et al.* [HESS Collaboration], 2008, Astropart. Phys., 29, 55 [Erratum-ibid. 2010, 33, 174]

Aharonian, F., [H.E.S.S.collaboration], 2009a, A&A, 503, 817

Aharonian, F., *et al.* [HESS Collaboration], 2009b, ApJ, 691, 175

Aharonian, F., *et al.* [HESS Collaboration], 2011, Astropart. Phys., 34, 608

Aharonian, F., *et al* [HESS collaboration], 2009b, A&A, 499, 273

Amsler, C., *et al.* (Particle Data Group), 2008, Phys. Lett. B, 667, 1

Anderhub, H., *et al.* [MAGIC Collaboration], 2009, ApJ, 702, 266

Baumgardt, H., Makino, J., & Hut, P., 2005, ApJ, 620, 238

Baumgardt, H., et al. 2009, MNRAS, 396, 2051

Berge, D., Funk, S., & Hinton, J., 2007, A&A, 466, 1219

Bergström, L., 2000, Reports on Progress in Physics, 63, 793

Bertone, G., & Fairbarn, M., 2008, Phys. Rev. D, 77, 043515

Bertone, G., Hooper, D., & Silk, J., 2005, Phys. Rept. 405, 279

Binney, J., & Tremaine, S., 1987, Princeton, NJ, Princeton University Press, 1987, 747 p.

Blumenthal, G. R., Faber, S. M., Flores, R., & Primack, J. R., 1986, ApJ, 301, 27

Bringmann, T., Bergstrom, L., & Edsjo, J., 2008, JHEP, 0801, 049

Brodie, J. P. & Strader, J., 2006, ARA & A, 44, 193

Bullock, J. S., *et al.*, 2001, MNRAS, 321, 559

Cohen, J. G., Kirby, E. N., Simon, J. D., & Geha, M., 2010, ApJ, 725, 288

Colbert, E., & Ptak, A., 2002, ApJS, 143, 25

Conroy, C., Loeb, A. & Spergel, D., 2010, arXiv:1010.5783

De Paolis, F., Gurzadian, V. G., & Ingrosso, G., 1996, A&A, 315, 396

Dewangan, G. C., *et al.*, 2005, ApJ, 635, 198

Dull, J. D., *et al.*, 1997, ApJ, 481, 267

Englmaier, P., & Gerhard, O., 2005, American Astronomical Society, 36th Annual Meeting, Santa Barbara, California, arXiv:astro-ph/0601679

Gebhardt, K., Pryor, C., Williams, T. B., Hesser, J. E., & Stetson, P. B., 1997, AJ, 113, 1026

Gerssen, J., *et al.*, 2002, AJ, 124, 3270

Gnedin, O. Y., Kravtsov, A. V., Klypin, A. A., & Nagai, D., 2004, ApJ, 616, 16

Gnedin, O. Y., & Primack, J. R., 2004, Phys. Rev. Lett., 93, 061302

Gondolo, P., & Silk, J., 1999, Phys. Rev. Lett., 83, 1719

Harris, W. E. 1996, AJ, 112, 1487 (Dec. 2010 update)

Islama, R., Taylor, J., & Silk, J., 2003, MNRAS, 340, 6471

Jesseit R., Naab, T., & Burkert, A., 2002, ApJ, 571, L89

Kabuki, S., *et al.* [CANGAROO Collaboration], 2007, ApJ, 668, 968

Kiselev, A. A., Gnedin, Y. N., Shakht, *et al.*, 2008, Astronom. Lett., 34, 529

Komatsu, E., *et al.* [WMAP Collaboration], 2009, ApJS, 180, 330

Kong, A. K. H., 2007, ApJ, 668, L139

Koushiappas, S. M., Bullock, J. S., & Dekel, A., 2004, MNRAS, 354, 292

Lanzoni, B., *et al.*, 2007, ApJ, 668, L139

McCutcheon, M. [VERITAS Collaboration], Proc. of the 31^{st} ICRC, Lodz, Poland, July 2009, arXiv:0907.4974 [astro-ph.HE]

Magorrian, J., *et al.*, 1998, AJ, 115, 2285

Mateo, M., 1998, Ann. Rev. Astron. Astrophys., 36, 435

Merritt, D., 2004, Phys. Rev. Lett., 92, 201304

Merritt, D., Harfst, S., & Bertone, G., 2007, Phys. Rev. D, 75, 043517

de Naurois, M., & Rolland, L., 2009, Astropart. Phys., 32, 231

Navarro, J. F., Frenk, C. S., & White, S. D. M., 1997 ApJ, 490, 493

Noyola, E., & Gebhardt, K., 2006, AJ, 132, 447

Noyola, E., Gebhardt, K., & Bergmann, M., 2008, ApJ, 676, 1008

Nucita, A. A., De Paolis, F., Ingrosso, G., Carpano, S., & Guainazzi, M., 2007, A&A, 763, 478

Peebles, P. J. E., 1984, ApJ, 277, 470

Prada, F., Klypin, A., Flix, J., Martinez, M., & Simonneau, E., 2004, Phys. Rev. Lett., 93, 241301

Pryor, C & Meylan, G., 1993, Astronomy Society of the Pacific, 50, 357

Pühlhofer, G., *et al.* [HEGRA Collaboration], 2003, Astropart. Phys., 20, 267

Rolke, W. A., Lopez, A. M., & Conrad, J., 2005, Nucl. Instrum. Meth., A551, 493

Rosenberg, J. L., Ashby, M. L. N., Salzer, J. J., and Huang, J.-S., 2006, ApJ, 636, 742

Spergel, D. N., *et al.* [WMAP Collaboration], 2007, ApJS, 170, 377

Spitzer, L., 1987, Princeton, NJ, Princeton University Press, 191 p.

Swartz, D. A., Ghosh, K. K., Tennant, A. F,. & Wu, K. W., 2004, ApJS, 154, 519

Ulvestad, J. S., Greene, J. E., & Ho, L. C., 2007, ApJ, 661, L151

Umbreit, S., Fregeau, J. M., and Rasio, F. A., 2008, Proc. of IAUS 246

Volonteri, M., Haardt, F., & Madau, P., 2003, ApJ, 582, 559

Wood, M., *et al.*, 2008, ApJ, 678, 594

Yungelson, L. R., van den Heuvel, E. P. J., Vink, J. S., Portegies Zwart, S. F., & de Koter, A., 2008, A&A, 477, 223

Zeldovich, Y. B., Klypin, A. A., Khlopov, M. Y., & Chechetkin, V. M., 1980, Sov. J. Nucl. Phys., 31, 664 [Yad. Fiz., 31, 1286].

Table 1: List of H.E.S.S. analysis cuts (de Naurois & Rolland 2009). The shower depth is the reconstructed primary interaction depth of the particle and the nominal distance is the angular distance of the image barycenter to the camera center.

Cut name	γ-event cut value
Shower goodness	≤ 0.4
Image charge (photo-electrons)	≥ 120
Reconstructed shower depth (radiation length)	$[-1, 4]$
Reconstructed nominal distance (°)	≤ 2
Reconstructed event telescope multiplicity	≥ 2

This preprint was prepared with the AAS LaTeX macros v5.2.

Table 2: Properties of the NGC 6388 and M 15 globular clusters used in this study.

	NGC 6388	M 15
Other Name	/	NGC 7078
RA, Dec coordinates (J2000)	$17^h36^m17.05^s$, $-44°44'05.8''$	$21^h28^m58.3^s$, $12°10'00.6''$
Galactic coordinates (l, b)	345.55°, -6.73°	64.8°, -27.1°
Distance (kpc)	11.5^a	10.0^c
Core radius r_c (pc)	0.4^a	0.04^d
Tidal radius r_t (pc)	25^a	30^c
Estimated mass ($M_\odot$)	10^6	5×10^5
Core stellar density ($M_\odot pc^{-3}$)	5×10^5	10^7
Central velocity dispersion v_{rms} (kms^{-1})	18.9 ± 0.8^b	10.2 ± 1.4^d

---

[a] Lanzoni et al.(2007)

[b] Pryor & Meylan (1993)

[c] Wood et al.(2008)

[d] Dull et al.(1997)

Table 3: Exposure time, mean zenith observation angle, number of ON events, number of OFF events, α ratio and 95% C.L. upper limits on the number of gamma-rays from the H.E.S.S. observations for NGC 6388 and M 15, respectively. See text for more details.

	NGC 6388	M 15
Exposure time^a (hours)	27.2	15.2
Mean zenith observation angle	22.9°	37.0°
N_{ON}	75	28
N_{OFF}	1754	719
α	26.5	26.6
$N_\gamma^{95\%C.L.}$	21.6	11.5

---

[a] After quality selection.

Table 4: Values of the los-integrated squared density averaged over the solid angle ($\bar{J}$) expressed in units of 10^{24} GeV^{2}cm^{-5}, for the different DM halo profiles. The integration solid angle is $\Delta\Omega = 5 \times 10^{-6}$ sr. The virial mass and concentration for the initial NFW profiles are given in brackets.

DM halo profile name	NGC 6388	M 15
Initial NFW ($M_{\rm vir}$, $c_{\rm vir}$)	2.1 (10^7 $M_\odot$, 60)	1.5 (10^7 $M_\odot$, 50)
AC NFW	1.3×10^4	4.3×10^3
IMBH NFW	2.2×10^4	/
Final	68	14

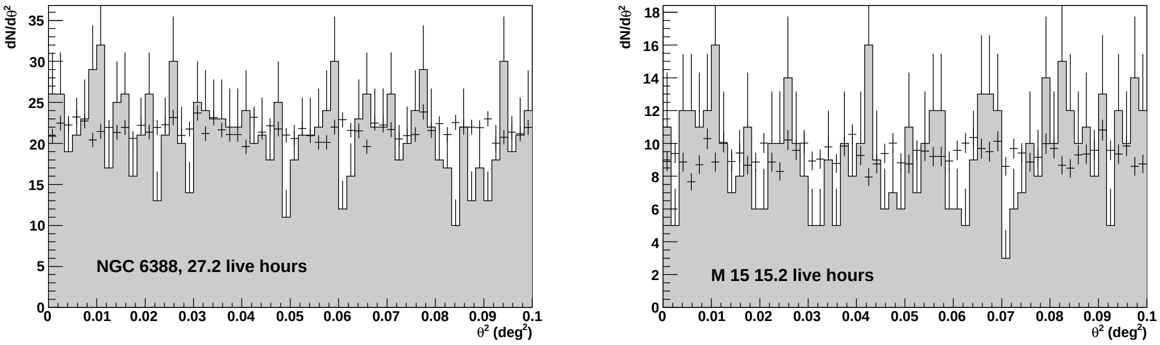

(a) NGC6388

(b) M15

Fig. 1.— θ^2 radial distribution of the ON (gray histogram) and normalized OFF (black crosses) events for gamma-ray like events from a 0.07° radius region around the target position for (a) NGC 6388 (RA=$17^{\rm h}36^{\rm m}17.05^{\rm s}$ and Dec=$-44^\circ44'05.8''$, J2000) and (b) M 15 (RA = $21^{\rm h}28^{\rm m}58.3^{\rm s}$ and Dec = $12^\circ10'00.6''$, J2000). The ON regions correspond to a maximum θ^2 of 0.005 deg^2. No significant excess is found in the ON region for NGC 6388 or M 15.

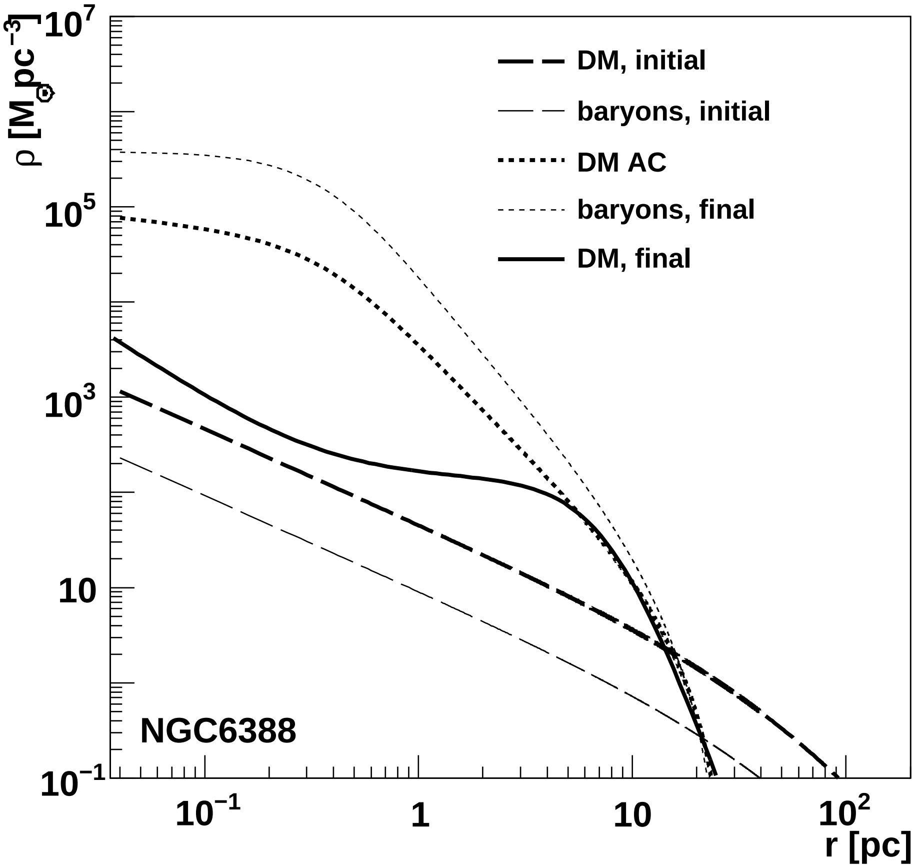

Fig. 2.— DM and baryonic mass density distributions in NGC 6388. The DM density before (thick dashed line) and after (thick dotted line) the adiabatic contraction by baryons is shown. The initial DM distribution follows a NFW profile with $M_{vir} = 10^7\,M_\odot$. The initial (thin dashed line) and final (thin dotted line) baryonic densities are displayed. The final DM density distribution after the effects of the adiabatic growth of the IMBH at the center of NGC 6388 and the kinetic heating by stars is presented (thick solid line). See text for more details.

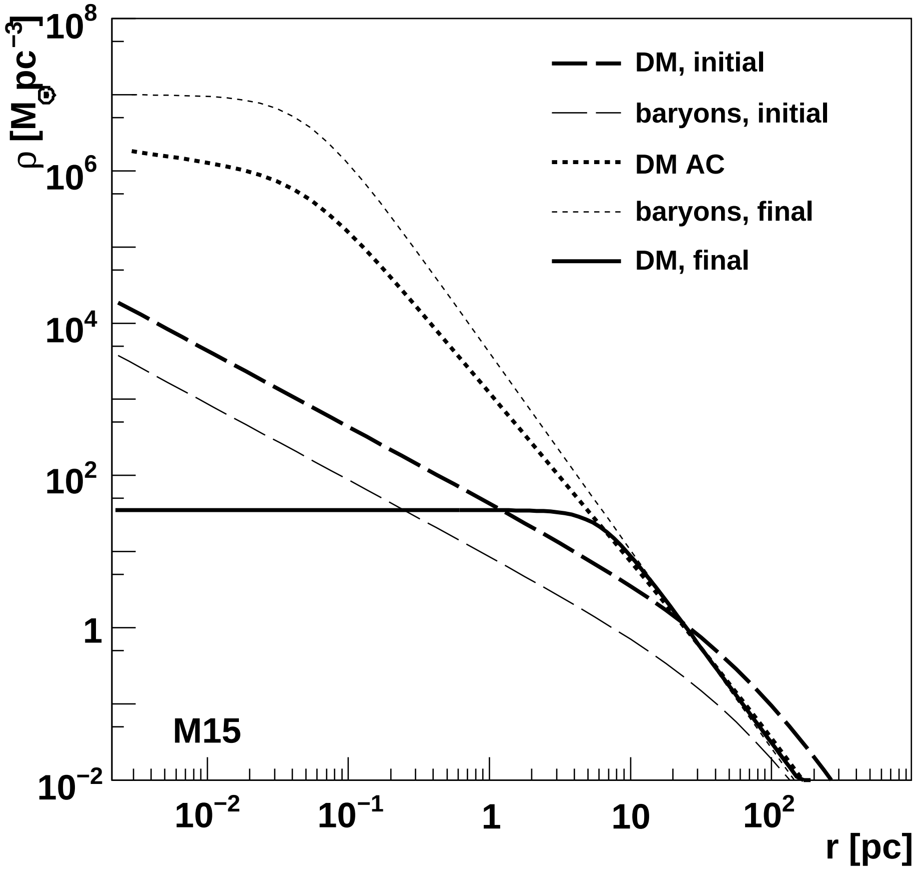

Fig. 3.— DM and baryonic mass density distributions in M 15. The DM density before (thick dashed line) and after (thick dotted line) the adiabatic contraction by baryons is shown. The initial DM distribution follows a NFW profile with $M_{\rm vir} = 10^7\,M_\odot$. The initial (thin dashed line) and final (thin dotted line) baryonic densities are displayed. The final DM density distribution after the effect of the kinetic heating by stars is presented (thick solid line). See text for more details.

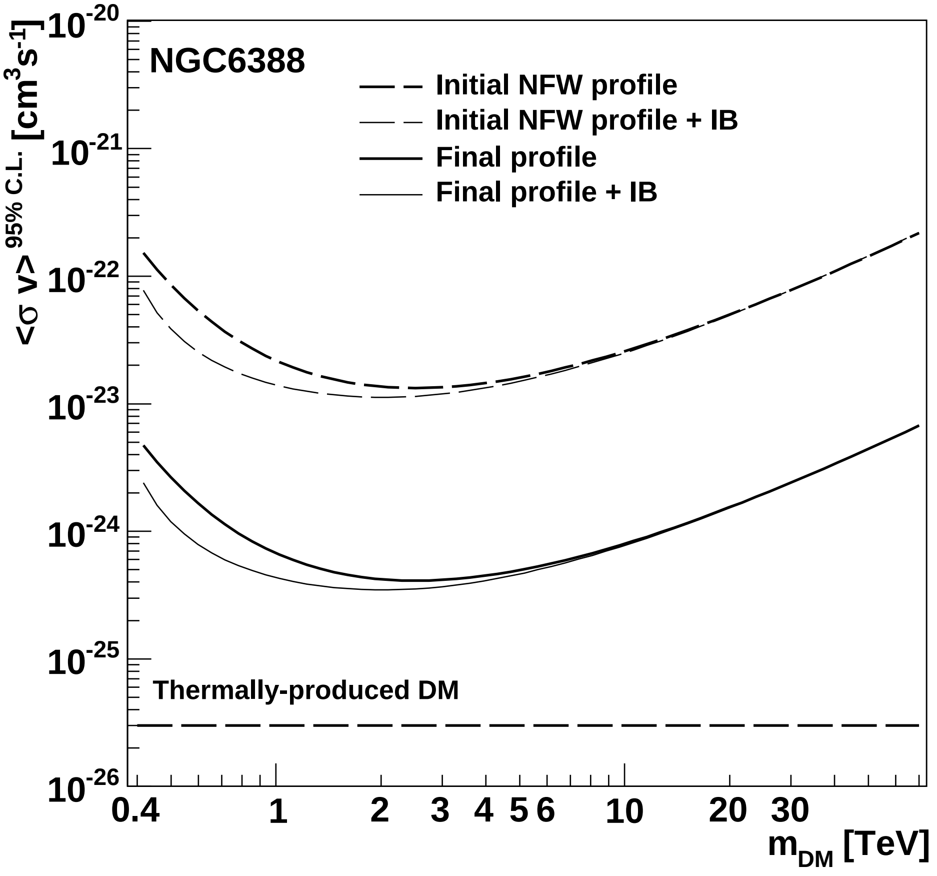

Fig. 4.— H.E.S.S. upper limits at 95% C.L. on the velocity-weighted annihilation cross section $\langle\sigma v\rangle$ versus the DM mass $m_{\rm DM}$ for the Galactic GC NGC 6388. DM halo profiles shown here correspond to the initial NFW profile (dashed thick line) and the realistic profile taking into account plausible astrophysical effects (solid thick line). The contribution from internal Bremsstrahlung and final state radiation to the annihilation spectrum is also shown (dashed/solid thin lines) for both profiles. The natural value of $\langle\sigma v\rangle$ for thermally-produced DM is also displayed (long-dashed line).

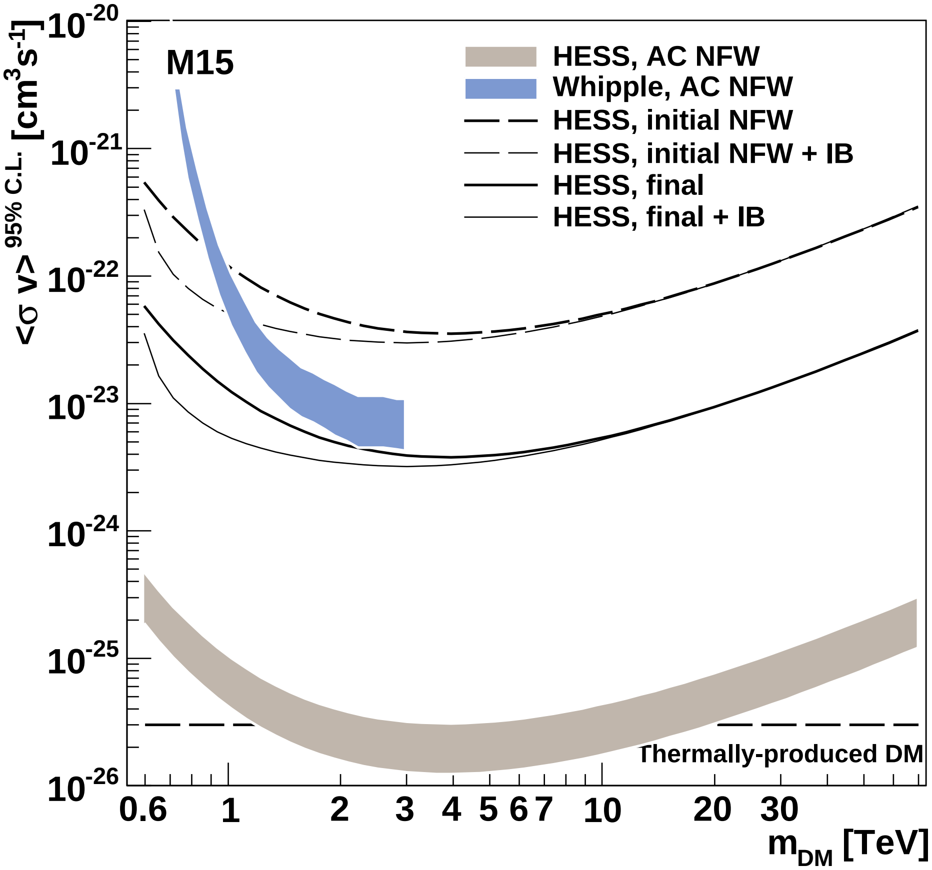

Fig. 5.— H.E.S.S. upper limits at 95% C.L. on the velocity-weighted anihilation cross section $\langle \sigma v \rangle$ versus the DM mass m_{DM} for the Galactic GC M 15. Three DM haloes are shown: the initial NFW profile (dashed thick/thin line), the NFW profile after DM adiabatic contraction by baryons (AC NFW) used in Wood et al. (2008) (gray area), and the final DM profile (solid thick/thin line). The effect of internal Bremsstrahlung is also presented (thin dashed/solid lines). The Whipple exclusion limits extracted from Wood et al. (2008) is also plotted (blue area). The natural value of $\langle \sigma v \rangle$ for thermally-produced DM is shown (long-dashed line).